International Journal of Biological Macromolecules 256 (2024) 128489

Contents lists available at ScienceDirect

International Journal of Biological Macromolecules

journal homepage: www.elsevier.com/locate/ijbiomac

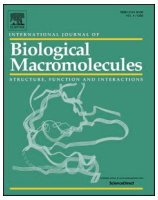

On the effect of pepsin incubation on type I collagen from horse tendon: Fine tuning of its physico-chemical and rheological properties

Luca Salvatore [a], Francesca Russo [b], Maria Lucia Natali [a], Zahra Rajabimashhadi [b], Sonia Bagheri [b], Claudio Mele [b], Francesca Lionetto [b], Alessandro Sannino [b], Nunzia Gallo [a,b,*]

[a] Typeone Biomaterials Srl, Via Europa 167, Calimera, 73021 Lecce, Italy
[b] Department of Engineering for Innovation, University of Salento, Via Monteroni, 73100 Lecce, Italy

ARTICLE INFO

Keywords:
Type I collagen
Equine collagen
Processing
Extraction, rheology, viscoelastic properties

ABSTRACT

Type I collagen is commonly recognized as the gold standard biomaterial for the manufacturing of medical devices for health-care related applications. In recent years, with the final aim of developing scaffolds with optimal bioactivity, even more studies focused on the influence of processing parameters on collagen properties, since processing can strongly affect the architecture of collagen at various length scales and, consequently, scaffolds macroscopic performances. The ability to finely tune scaffold properties in order to closely mimic the tissues' hierarchical features, preserving collagen's natural conformation, is actually of great interest. In this work, the effect of the pepsin-based extraction step on the material final properties was investigated. Thus, the physico-chemical properties of fibrillar type I collagens upon being extracted under various conditions were analyzed in depth. Correlations of collagen structure at the supramolecular scale with its microstructural properties were done, confirming the possibility of tuning rheological, viscoelastic and degradation properties of fibrillar type I collagen.

1. Introduction

Type I collagen is one of the most abundant structural proteins in mammals, and it is found in the extracellular matrix (ECM) of tissues where it performs not only structural support but also highly specialized regulatory functions, that are involved in tissue development and repair/regeneration processes [1–4]. The presence of natural binding sites for cells, the consequent high capacity of cell adhesion and the important role in cell signaling, its intrinsic bioactivity, biocompatibility, biodegradability, and low immunogenicity, made type I collagen one of the most suitable biomaterials for healthcare related applications [5–12].

Differently from other proteins, type I collagen is not a single protein but belongs a family of proteins (i. e., collagens family) that share a particular, unique, structure. In particular, type I collagen is composed of three left-handed polyproline-II chains (commonly called 'α chains') that assemble in a right-handed triple helix [13,14]. Type I collagen unit is composed of two identical α1 chains and one, slightly different, α2 chain [15]. Each α chain consists of the repetition of a sequence of three amino acids (Gly-X-Y) n where the first position is always occupied by glycine (Gly), while the X position is usually proline and the Y position hydroxyproline. Gly repeats itself every three amino acid residues along the entire length of the chain (consisting of about 1000 amino acids [14]. Its position plays a key role in the packaging of the three α chains [16]. Hydroxyproline comprises about 10–14 % of the amino acid composition of collagen and together with proline, stabilizes the triple helix through the formation of hydrogen bonds [15].

Type I collagen is a fibril forming protein. Indeed, the triple-helical units (length ≈300 nm, diameter ≈1.5 nm) spontaneously self-assemble parallel one to another (i.e., fibrillogenesis process) in fibrils (length ≈μm, diameter ≈100 nm) with a staggering of about 67 nm (i.e., D-periodicity or D-banding) [13,17]. Fibrils in turn assemble in fibers of a length of about millimeters and a diameter of about 10 μm [18]. Then, collagen fibers randomly (i.e., skin) or preferentially (i. e., tendon) arrange in tissues to provide them with the appropriate structural architecture and functional integrity.

* Corresponding author at: Department of Engineering for Innovation, University of Salento, Via Monteroni, 73100 Lecce, Italy
E-mail addresses: l.salvatore@typeone.it (L. Salvatore), francesca.russo@unisalento.it (F. Russo), m.natali@unisalento.it (M.L. Natali), zahra.rajabimashhadi@unisalento.it (Z. Rajabimashhadi), sonia.bagheri@unisalento.it (S. Bagheri), claudio.mele@unisalento.it (C. Mele), francesca.lionetto@unisalento.it (F. Lionetto), alessandro.sannino@unisalento.it (A. Sannino), nunzia.gallo@unisalento.it (N. Gallo).

https://doi.org/10.1016/j.ijbiomac.2023.128489
Received 6 July 2023; Received in revised form 10 November 2023; Accepted 27 November 2023
Available online 1 December 2023

Accordingly, type I collagen extracted from highly hierarchically organized tissues (i.e., bovine, equine, porcine or ovine tendons) still retains a partial lateral packing arrangement despite the disruptive treatments of the extraction processes compared to collagen isolated from tissues with a random organization [19–21]. The partial retention of fibrous structures allows to obtain materials and reconstituted devices with enhanced properties (i.e., higher resistance to degradation and mechanical stress) compared to homologues obtained from type I collagen derived from skin [2,20,22]. Due to this, tendons derived collagens are preferred to skin derived collagens for the manufacturing of implantable collagen-based devices.

Among them, as in detail reported by Gallo et al., collagen derived from horse tendons was revealed to have numerous advantages [2]. In brief, compared to other animal extraction sources, it was found to be almost free from zoonosis transmission risks, to have the highest sequence homology with human collagen (about 95.6 %) after bovines, to not be immunogenic, and to have the highest hydroxyproline content, and thus to be intrinsically more resistant than other collagens [2]. Moreover, it has been documented that the natural strict hierarchical organization of equine tendon, compared to tissues from other mammals, allows for better collagen native structure after the extraction process and the following processing [19], suggesting its great potential in the biomedical field where the preservation of natural binding sites for cells and of its intrinsic bioactivity is of fundamental importance.

However, it should be accounted that collagen processing, from the extraction process to the sterilization of the end product, strongly influences its conformational structure and thus its biological, physicochemical, and mechanical performances [1]. Obviously, process parameters of all steps have an effect on material properties. Due to this, they could be varied and customized as wanted in order to manufacture products with tunable properties in terms of morphology, viscoelasticity, rheology, degradation resistance and biological response. However, it is of fundamental importance to preserve collagen bioactivity, which is ensured by the retention of its natural conformation. The collagen molecule is indeed characterized by integrin binding sites (i.e., the “GFOGER” sequence) which are fundamental for cell adhesion, interaction, proliferation, and differentiation [23,24]. Recently, scientific and industrial research moved their interest toward the possibility of tuning product properties in the preliminary steps of their production process with the aim of developing customized devices without resorting to chemical crosslinker or other biomaterials. This trend was due to the even more strict regulation for the approval of chemically crosslinked devices that, because of their potentially harmful byproducts, were usually not approved for clinical applications. Thus, novel strategies plan to act on the upstream phases of the devices production process, which are the extraction steps (i.e., enzyme concentration, pH, temperature, homogenization), the material preliminary processing (i.e., fibrillogenesis, homogenization, sonication) and the manufacturing (i.e., technique, material concentration, pH, temperature). Among them, the extraction step plays a fundamental role since it influences all successive material manufacturing phases. In particular, the extraction key phase is the so called ‘enzymatic treatment’, which allows collagen fiber to gradually disassemble [25–27]. By tuning exposure time, kind and concentration of enzyme, temperature, and pH, it is possible to obtain different types of reconstituted collagen, from the native protein extracts (i.e., fibers, fibrils) to single protein unit (i.e., triple helix), to peptides. Many enzymes were used to isolate collagen and its derivates, including trypsin, chymotrypsin, alcalase, bromelain, collagenase, ficin, flavourzyme, neutrase, pancreatin, thrombin, papain, and others [28–33]. However, the most widely used for native collagen extraction is pepsin that cleaves collagen non-helical telopeptide regions without disrupting its triple-helical structure [34,35]. Thus, the use of pepsin in determined experimental conditions, compared to other enzymes, allows for the preservation of collagen native structure thanks to its higher affinity to unfolded proteins rather than folded. Thereafter, it allows to disaggregate collagen microfibrils or tropocollagen from collagen fibers without destroying them or turning them into low molecular weight peptides. Since collagen bioactivity is strictly related to its hierarchical organization, the use of pepsin allows to preserve its native biological functions by retaining its natural structural conformation. For this reason, pepsin is widely used for native collagen extraction.

However, while the effect of pepsin on collagen extracted from other sources was investigated [32,33,36–42], to the best of our knowledge, no works on the effects of pepsin-based extraction on the final properties of native equine tendon derived collagen, a recently available collagen with appealing properties, were already published. Thus, in this work, the effect of the variation of some parameters of the pepsin-based extraction step on the material final properties was investigated. In particular, the influence of pepsin concentration, temperature and homogenization were in depth investigated with the aim to assess the capability to tune some material properties according to the desired application. The identity and the naiveness of the extracted protein were assessed by Poly-Acrylamide Gel Electrophoresis in the presence of Sodium Dodecyl Sulphate (SDS-PAGE). The conservation of functional groups was assessed by the 2,4,6-trinitrobenzenesulphonic acid (TNBS) test. The presence of collagen fibers and their characteristics was investigated by means of Atomic Force Microscopy (AFM). Moreover, the collagen secondary structure was in depth analyzed by Fourier Transform Infrared Spectroscopy (FT-IR). The thermal behavior was determined by Differential Scanning Calorimetry (DSC). Then, collagen suspensions' rheological properties and thin substrates' mechanical properties were investigated. Lastly, the results of all analyses were correlated with in vitro degradation resistance in physiological-like conditions.

2. Materials and methods

2.1. Materials

Type I collagen samples isolated from equine tendons were provided by Typeone Biomaterials S.r.l. (Calimera, Italy). Pepsin from porcine gastric mucosa (P7125), TNBS, phosphate buffered saline (PBS), sodium dodecyl sulfate (SDS), glycerol, Collagenase from *Clostridium histolyticum* (C0130), and acrylamide/bisacrylamide solution (37.5,1) were purchased from Merk (Darmstadt, Germany). Bromophenol blue, Coomassie brilliant blue R-250, ammonium persulfate, *N*,*N*,*N*,*N*-tetramethyl ethylene diamine (TEMED), and 2-mercaptoethanol were purchased from Bio-Rad Laboratories (Hercules, CA, USA). Distilled water was obtained from Merck KGaA's Millipore Milli-U10 water purification plant (Darmstadt, Germany). If not otherwise stated, other analytical grade chemical reagents were purchased from Merk (Darmstadt, Germany).

2.2. Collagen extraction

As well known, most collagen extraction methods used in industrial practice basically constist of a multistep process including four main phases, that are: i) cleaning and size reduction; ii) removal of non-collagenous components; iii) collagen extraction via acidic and/or enzymatic treatment; iv) recovery of the isolated material (Fig. 1).

Type-I collagen formulations used in this work were produced by Typeone Biomaterials Srl by means of an optimized (proprietary) extraction process, starting from the equine tendon as source tissue, according to ISO standards of quality. The effect of the variation of some processing parameters of the enzymatic extraction step on the material final properties was investigated. In particular, five conditions were analyzed, comprising three pepsin concentrations, two temperature values and a homogenization step, as summarized in Table 1. The pepsin concentration was calculated against the collagen content (Table S1). The homogenization step was performed by mean of an IKA T25 Digital Ultra Turrax overhead blender (IKA® - Werke GmbH & Co., KG, Breisgau, Germany) at 10000 rpm for 5 min at 4 °C before pepsin incubation

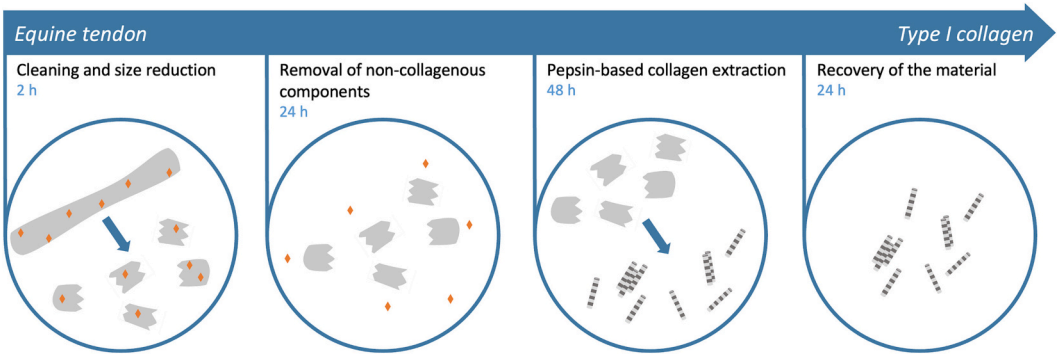

Fig. 1. Type I collagen extraction from horse tendon process. Schematic procedure of collagen isolation protocol consisting in four main phases.

Table 1
Sample type and applied treatment.

Sample	Treatment
A	Pepsin 5 %, 15 ± 5 °C
B	Pepsin 10 %, 15 ± 5 °C
C	Pepsin 50 %, 15 ± 5 °C
D	Homogenization, pepsin 5 %, 15 ± 5 °C
E	Pepsin 5 %, 30 ± 5 °C

in order to disassemble and/or disperse collagen fibrils. As regards temperature, 15 °C was chosen in order to decelerate (and thus to better control) pepsin activity, while 30 °C was chosen in order to near pepsin optimal working temperature, that is body temperature. The exposure time (48 h) and the pH value (2.5) were the same for all experimental conditions. Other different pepsin content and temperature conditions were preliminarly investigated but, since their effect was not significant, there were not reported in this work. After the enzymatic treatment, collagen lots were precipitated at a neutral pH (7.4), washed trice with distilled water by centrifugation (9000 rpm, 20 min, 10 °C) and freeze-dried. Then, fibrillar, insoluble, dry collagen flakes were obtained and stored at 4 °C in the darkness until use.

An in-depth analysis of the properties of the fibrillar type I collagen lots was done both on collagen suspensions and air-dried films. These two physical forms allowed to investigate several aspects of the investigated fibrillar type I collagens. Indeed, molecular weight, thermal behavior and rheological properties were assessed by analyzing collagen suspensions while free amino groups, structural organization, surface characteristics, mechanical properties and the behavior in physiological-like environment (swelling degree, degradation resistance) were assessed by analyzing collagen air-dried films.

The collagen suspensions were prepared by resuspending dry collagen flakes in acetic acid 0.5 M at a final concentration of 1 % (*w/v*) and magnetically stirring them for 4 h at 10 °C to avoid collagen denaturation. All suspensions were degassed by centrifugation at 5000 rpm for 5 min at 10 °C before use.

The collagen air-dried films were prepared according to a previously optimized protocol [43–45]. In particular, degassed 1 % (w/v) collagen suspensions were cast in Petri dishes. Then, air drying was performed in a laminar flow hood for 72 h at room temperature [44]. Following air drying, collagen films were peeled from Petri dishes and stored at 4 °C in the darkness until use.

2.3. Molecular weight and purity

Collagen purity and molecular weight were evaluated by SDS-PAGE using a Mini-Protean Tetra Cell System (Bio-Rad Laboratories, Inc., Hercules, CA, USA). Collagen suspensions were subjected to reductive treatment with Laemmli buffer (62.5 mM Tris-HCl pH 6.8, 10 % glycerol, 2 % SDS, 0.01 % blue bromophenol, 5 % β-mercaptoethanol) and 2 M Urea to disaggregate collagen fibrils at 50 °C for 1 h [44,46,47]. After 1 min of centrifugation at maximum speed, few microliters of supernatant were withdrawn and loaded into the wells of two electrophoretic polyacrylamide gels with different mesh sizes. The first was made of 5 % stacking gel, and 12 % resolving gel. The second was made of 5 % stacking gel, and 6 % resolving gel. The electrophoretic run was performed in the presence of protein standards with precise molecular weights ranging from 10 to 250 kDa. The electrophoretic run was done at 70 *V* for about 30 min and then at 120 V for about 2.5 h. At the end of the run, the gel was stained with a Coomassie Brilliant Blue rapid staining solution (0.8 % Coomassie Brilliant Blue G250, 0.04 M HCl). In particular, the gel was rinsed with tap water twice, soaked in the pre-heated staining solution (80 °C) for 45 min, washed with distilled water and then acquired [43,48]. The analysis was done in triplicate. The revealed protein bands were analyzed by mean of the software GelAnalyzer 19.1 (www.gelanalyzer.com, accessed on 01 February 2023) by Istvan Lazar Jr., PhD and Istvan Lazar Sr., PhD, CSc for protein subunits ratio and molecular weight determination.

2.4. Free amino groups extent

The number of free primary amino groups was determined by a test based on the use of TNBS, following an already optimized protocol [49–51]. Approximately 3 mg of collagen air-dried films [43–45] were added with 0.5 mL of 4 % (*w/v*) $NaHCO_3$ in hermetically sealed test tubes. After 30 min, 0.5 mL of a freshly prepared 0.05 % (w/v) TNBS was added. The reaction mixture was incubated at 40 °C for 2 h. Then, after the addition of 1.5 mL of 6 M HCl, samples were incubated at 60 °C for 90 min. Subsequently, the reaction mixture was diluted with 2.5 mL of distilled water and the absorbance at 410 nm was measured with a UV–visible spectrophotometer when the reaction mixture reached room temperature. A calibration line obtained with serial dilutions of 0.1 mg/mL glycine was carried out, in which the absorbance was correlated to the concentration of free amines. The test was done in triplicate for each sample type.

2.5. Structural organization

The collagen samples' structural organization was analyzed by FT-IR by means of the FTIR-6300 spectrometer from Jasco GmbH (Pfungstadt, Germany). Samples were prepared by casting and air-drying on germanium IR lenses 0.1 mL of three-fold diluted of 1 % collagen suspensions. Absorption spectra in absorbance mode were recorded in the range 4000–400 cm^{-1} with a resolution of 4.0 cm^{-1}, 64 scans. Each spectrum was analyzed using Origin software from Origin Lab Corporation (Northampton, MA, USA).

2.6. Surface characteristics

The surface morphology was characterized through a MultiMode 8

AFM system (Bruker, Champs sur Marne, France) on air-dried collagen films. AFM imaging was carried out in Peak Force Quantitative Nanomechanical Mapping (QNM) mode with scanasyst-air probe, using a silicon tip on nitride lever cantilever with the spring constant of 0.4 N/m (Bruker, nominal length 115 μm, nominal tip radius 2 nm) [43–45]. The scanning parameters were optimized to obtain high-quality images of the surface topography. The scan sizes were set at 10 × 10 μm^2, 5 × 5 μm^2, 1 × 1 μm^2, the scanning rates in the 0.640–0.574 Hz range, and the resolution at 512 lines per scan. Nanoscope Analysis v.1.5 software was applied for the AFM data processing, and for the roughness measurements. The roughness Rq was calculated as the root mean square of z-channel variations with respect to the mean height value calculated on the overall image area. Rq of each sample was determined as the average value calculated in ten different areas of 1 × 1 μm^2.

2.7. Rheological properties

The viscoelastic properties of collagen suspensions were investigated by DMA using a parallel plate ARES rheometer (Rheometric Scientific, Piscataway, NJ, USA). The collagen suspensions were loaded between two parallel plates of 25 mm diameter, with a distance of 0.5 mm. In order to determine the linear viscoelastic range (LVR) and the critical strain, oscillatory strain sweep measurements at an oscillation frequency of 1 Hz in the strain interval from 0.01 % to 100 % were carried out. Then, frequency sweeps in the LVR between 0.01 Hz and 16 Hz were applied over a linear strain (1 %) at 20 °C. The critical strain γ_{crit} was also used for calculating the cohesion energy E_c:

$$E_c = \frac{1}{2}\,\gamma_{crit}^2\,G'_{crit} \tag{1}$$

where G'_{crit} is the value of the storage modulus at the critical strain γ_{crit}. The cohesion energy is related to the energy required for the formation of physical crosslinks between the polymer chains [52,53]. Rheological measurements were carried out in steady mode in the shear rate range between 0.1 s^{-1} and 1000 s^{-1} at 20 °C. At least three measurements were carried out for each sample type.

2.8. Thermal behavior

Thermal analysis was performed both on collagen suspension and air-dried film samples using a Mettler DSC1 Differential Scanning Calorimeter (Mettler Toledo, Greifensee, Switzerland). Collagen suspensions or films of about 5–10 mg were equilibrated in hermetically sealed aluminum pans at the starting temperature of 10 °C for 10 min and then heated at 5 °C/min from 10 °C to 100 °C, in a nitrogen atmosphere [48,54]. At least three measurements were carried out for each collagen type. The denaturation temperature (Td) was determined as the peak value of the corresponding endothermic phenomenon. The denaturation enthalpy (ΔH) was calculated with respect to the collagen mass of the sample.

2.9. Swelling degree

The ability of collagen substrates to absorb liquids was assessed by the calculation of their swelling degree. Air-dried films of about 3.0 × 3.0 × 0.05 cm were weighed (40–50 mg) and soaked in PBS 1×. After removing the excess water by blotting them on filter paper, wet films were weighed at a fixed time point. The degree of swelling (SD%) was calculated according to the following Eq. (2) [43,45,55]:

$$SD\% = \frac{W_w - W_d}{W_d} \times 100 \tag{2}$$

where W_d is the dry film weight and W_w is the wet film weight at prefixed time points. The test was done in triplicate for each sample type.

2.10. Mechanical properties

The tensile tests were carried out with a ZwickLine universal testing machine (Zwick/Roell, Ulm, Germany) equipped with a 100 N load cell. Air-dried collagen films [43–45] were cut approximately 2.5 cm × 0.5 cm and equilibrated in PBS 1× at room temperature for 2 h. Then, uniaxial tensile tests were performed under displacement control till failure with a preload of 0.1 N and a test speed of 0.1 mm/s [43]. The Young's modulus (E), the stress at break (σ_{max}) and the strain at break (ε_r) were analyzed with the software Microsoft Excel (Microsoft, WA, USA). The width and thickness of the hydrated films were measured with a Dino-Lite digital microscope (AnMo Electronics Corporation, New Taipei City, Taiwan). Each sample was tested in triplicate.

2.11. In vitro degradation resistance

The stability test was performed to assess the resistance to degradation of collagen samples under physiological-like conditions. Air-dried collagen films of 3 cm × 3 cm were weighted and incubated in 5 mL PBS 1× at 37 °C in the presence and in the absence of collagenase 0.5 U/mL. For each prefixed time point, few microliters were withdrawn and used to determine the amount of protein degraded using the colorimetric test with bicinchoninic acid (BCA) (QuantiProTM BCA Assay Kit, Sigma Aldrich).

2.12. Statistical analysis

The statistical significance of the experimental data was studied using the *t*-Student test. Data were expressed as mean ± the standard deviation. The differences were considered significant at $p < 0.05$.

3. Results

3.1. Molecular weight and purity

Type I collagen protein composition and purity were assessed by SDS-PAGE. The electrophoretic patterns of samples A-E were reported in Fig. S1 and in Fig. 2 and were found to be comparable to that one reported in our previous study [44]. The electrophoretic run on the 12 % polyacrylamide gel was performed to assess collagen purity and integrity while the electrophoretic run on the 6 % polyacrylamide gel was performed to clearly assess eventual molecular weight or intensity profile differences among samples. As expected, all samples were characterized by the two typical bands of collagen α1 (≈130–140 kDa) and α2 (≈110–120 kDa) chains [44,56]. Moreover, β (cross-links between two α-chains) and γ (cross-links between three α-chains) chains were also revealed. As shown in Fig. S1, non-collagen protein bands were not observed, indicating the purity of all collagen samples and the preservation of their protein structure. Thus, the low and poor collagen hydrolyzing activity of pepsin [32] was revealed to be effective for native collagen isolation. These results demonstrated also that the selected extraction conditions with pepsin were capable of cleaving collagen without affecting the native α chain length.

In order to assess molecular weight or intensity profile differences among samples, samples were run also on 6 % polyacrylamide gels. As shown in Fig. 2, although the samples molecular weight seemed to be almost the same (i.e., γ = 326 ± 17 kDa, β = 241 ± 5 kDa, α1 = 120 ± 2 kDa, α2 = 107 ± 1 kDa), a different band intensity was detected, attributable to the different soluble collagen extent. In particular, β and γ chain intensity was found to decrease with the pepsin concentration, according to the literature [32]. Indeed, a reduction of about 27 % of β + γ chains was registered in sample B, and of about 45 % in sample C, compared to sample A. Clear was also the impact of the introduction of a preliminary homogenization step, that induced a β + γ chains reduction of about 34 % in sample D, allowing for a higher protein aggregates disassembly with a lower content of pepsin. A high β + γ chains

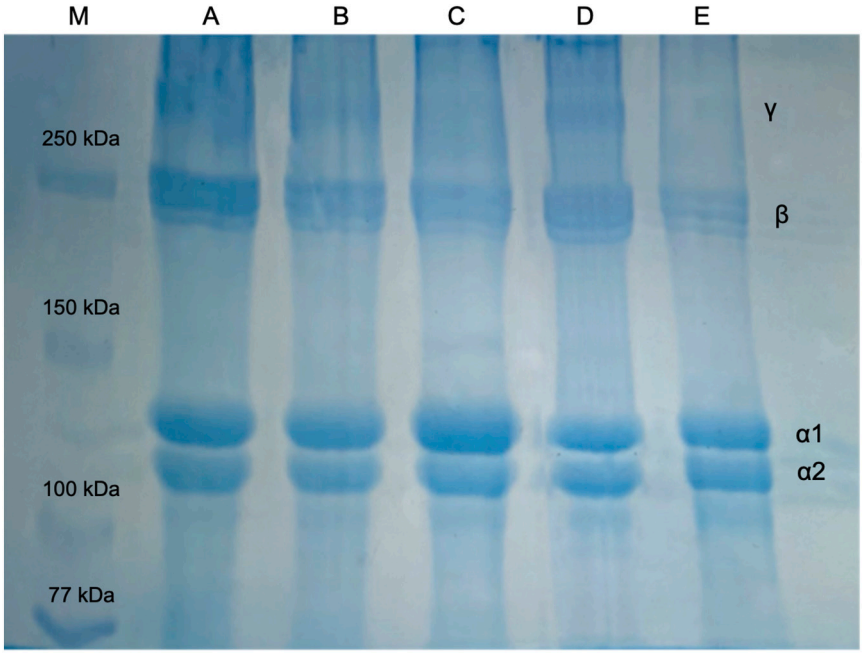

Fig. 2. Collagen samples electrophoretic pattern. Comparison of the electrophoretic pattern of collagen samples on 6 % polyacrylamide gel in comparison with standard protein markers (M), confirming the presence of α1 and α2 chains, besides of β and γ chains.

disaggregation was obtained also by increasing the working temperature up to 30 °C and maintaining the pepsin concentration low. Indeed, in sample E, a reduction of β + γ chains content of about 41 % was registered. As regards, α1 and α2 chains, a similar and inverse, behavior was observed. An increase in their band intensity was registered according to pepsin concentration [57]. In particular, an increase of α1 + α2 content of about 12 % was observed in sample B and of about 22 % in sample C, compared to sample A. The addition of a homogenization step or the increase of the working temperature was revealed to be able to increase the α1 + α2 content of about 18 %.

3.2. Structural organization

FTIR analysis was performed in order to assess the collagen nature after the extraction process. Air-dried 1 % (*w/v*) collagen suspensions were not optically transparent and absorbance values registered were up to 2. To acquire significative data, diluted collagen suspensions were required. In particular, after several concentration analysis attempts, the 0.3 % (w/v) dilution allowed to acquire accurate absorbance spectra. As reported in Fig. 3, all samples exhibited the typical spectra of type I collagen [44,45,48,58–61]. The peaks of amide I, amide II, and amide III of type I collagen were clearly detected and found in the same positions (Table 2). The amide I, associated with C═O hydrogen-bonded stretching, was found at 1653–1654 cm^{-1}. The amide II, due to C—N stretching and N—H in-plane bending of the amide linkage, peaked at 1554–1556 cm^{-1}. The amide III, attributed to the N—H bending coupled with CH_2 wagging and C—N stretching, was found at 1242–1255 cm^{-1}. The wavenumber difference between Amides *I* and II peaks was equal to or lower than 100 cm^{-1}, indicating that the triple helical structure was maintained [62]. Moreover, the intensity ratio of Amide III (1242 cm^{-1}) and CH_2 (1450 cm^{-1}), which indicates collagen triple helical content, was revealed to be different among sample type. In particular, it was found to be higher than 1 for samples A (2.5), B (2.2) and D (2.3), and lower than 1 for samples C (0.86) and E (0.96), confirming the higher preservation of the triple helical content of the first samples and the partial destruction of the latter [63,64]. Thus, according to Feng et al. [36], pepsin hydrolysis did not affect the collagen triple helical structure.

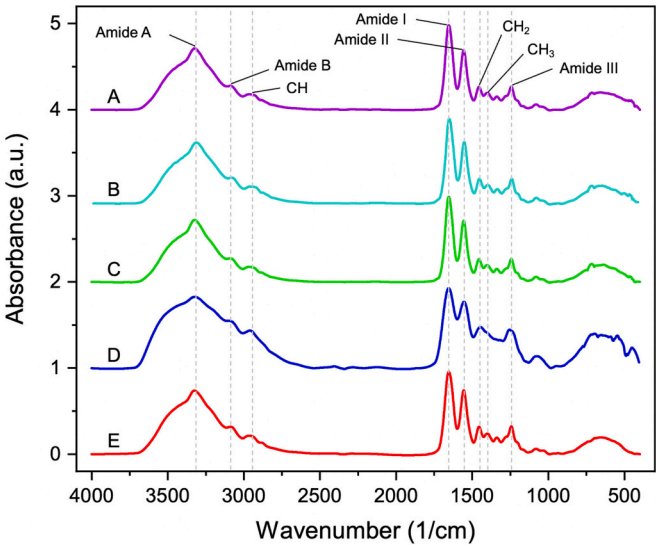

Fig. 3. FT-IR spectra of collagen films. The principal peaks identified were that one characteristic of type I collagen, that were amide I, amide II, amide III, amide A and amide B.

Table 2
FT-IR peak location and assigment of collagen samples.

Peak wavenumber (cm^{-1})	A	B	C	D	E
Amide I	1653	1654	1654	1654	1653
Amide II	1556	1556	1556	1554	1556
Amide III	1242	1242	1242	1245	1242
Amide A	3324	3320	3322	3322	3326
Amide *B*	3089	3089	3089	3100	3087

Besides these three principals contributions, other peaks were present and were attributed to the: i) N—H stretching coupled with intramolecular H-bond (Amide A, 3320–3326 cm^{-1}), ii) N—H bending

(Amide *B*, 3087–3100 cm^{-1}), iii) $-CH_3$ wagging and deformation (1399–1401 cm^{-1}), iv) $-CH_2$ stretching of the glycine backbone (1450–1455 cm^{-1}), v) and of $-CH_3$ stretching (2959–2968 cm^{-1}) [58,65,66].

The presence of all peaks attributable to type I collagen confirmed the protein nature and that chosen collagen extraction processes partially affected its triple helical structural organization, which was found to be almost preserved. However, despite the general high preservation of collagen unit triple helical structure, no considerations could be made on the collagen fiber preservation degree from this analysis.

3.3. Free amino groups extent

The TNBS test was performed to measure the number of primary amines present in collagen samples after modification of the standard extraction process. As can be seen in Fig. 4, the performed enzymatic treatments did not affect collagen formulations free amino group content since no significant differences were revealed among most of the samples, except between sample B and sample C where an increase of free amino groups was registered with pepsin concentration.

3.4. Surface characteristics

The AFM images of dry equine tendon collagen films were reported in Fig. 5, where randomly oriented collagen fibrils were visible, as indicated by white arrows. The inset in each sample image, showing a single collagen fiber, was used for the determination of D-band periodicity. This periodicity is considered a characteristic property of all fibrils-forming collagens and it plays a crucial role in the interactions between cells and collagen [67]. As reported in Fig. 6, all samples exhibited a D-banding value of about 60–70 nm, with no statistically significant differences ($p > 0.2$). According to the literature [17,43,67,68], these results indicated that the extraction process did not significantly alter the collagen fibrillar structure.

Beyond collagen D-banding, the width and surface of fibrillar zones and roughness range in each collagen sample were investigated. Although the fiber diameter was found to be almost the same in all samples ($p > 0.1$), a significant difference was observed in the measured number of fibers for the area unit. The highest value was observed in sample B at 59.0 ± 1.0 %, followed by sample D at 51.5 ± 1.5 %. Samples E, A, and C presented more or less the same values, 47.5 ± 0.7 %, 46.0 ± 2.2 %, and 43.5 ± 2.1 %, respectively. It should also be noted that fibrillar zones were not observed in all samples with the same color

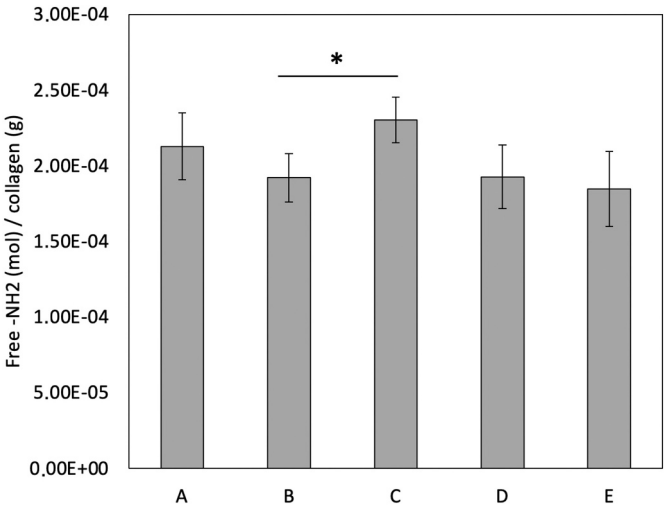

Fig. 4. Quantification of collagen free amino groups. Data were expressed as moles of free amino groups per gram of collagen (x10^5) and were measured by the TNBS test. (*, $p < 0.05$).

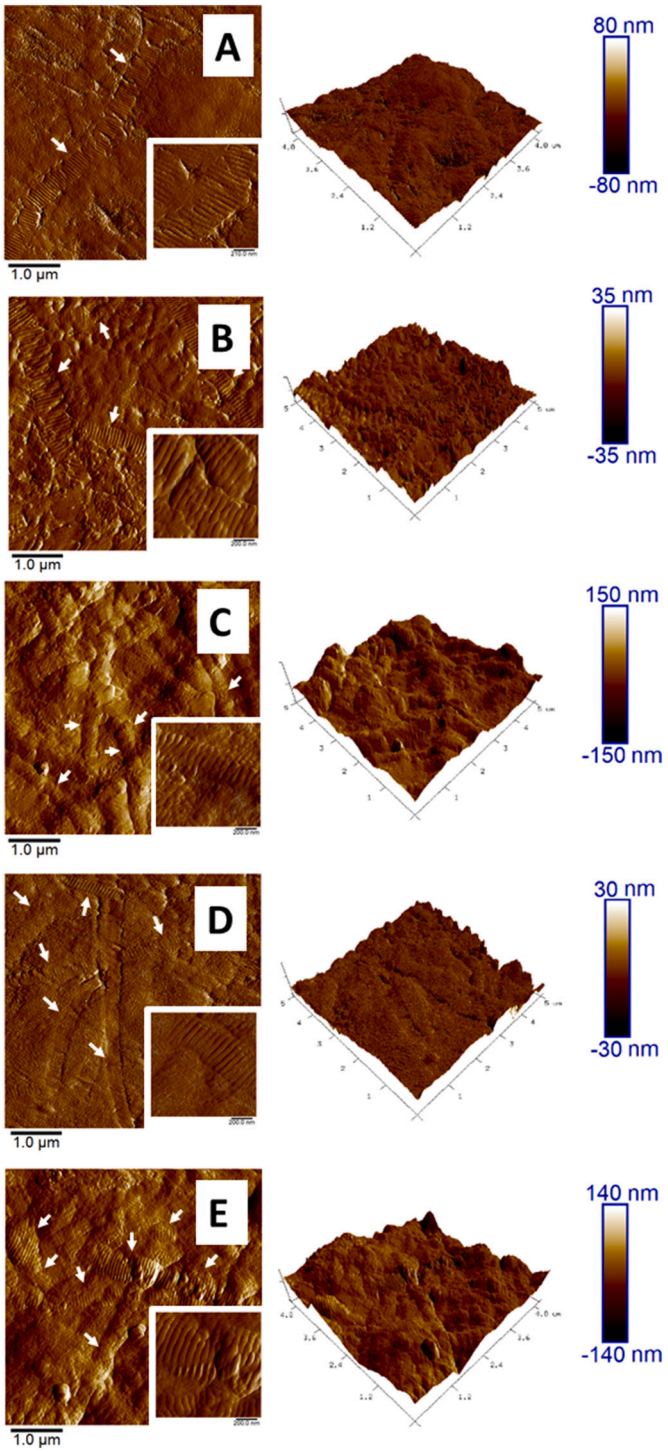

Fig. 5. AFM images of collagen films. Samples are reported at 5 × 5 μm^2. The inset in each sample was acquired in the 1 × 1 μm^2 image size.

contrast. The reason for this is the difference in the surface roughness of the samples. For example, in sample D, where the fibrillar area is very blurred, the maximum and minimum roughness is very low.

As regards the roughness, samples A, B and D presented the lowest values, that was found to be significantly different from that of samples C and E ($p < 0.05$).

3.5. Rheological properties

The evolution of the storage shear modulus (G') as a function of shear

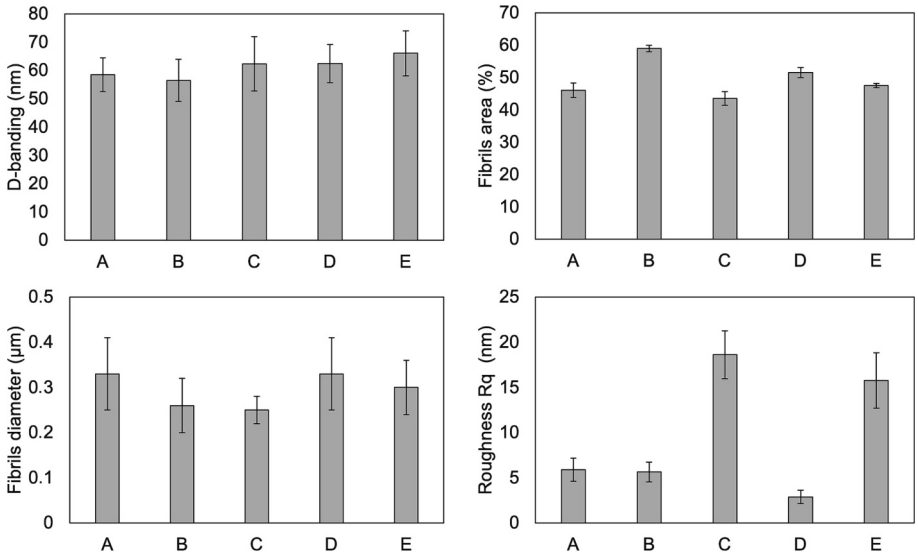

Fig. 6. Morphological properties of equine collagen films obtained from AFM analysis. Fibers properties were analyzed in terms of D-banding, fibrils area, fibrils diameter, and roughness.

strain in a dynamic strain sweep test at 1 Hz and 20 °C is reported in Fig. 7. At very low strain values, G' was higher than the loss modulus (G") for all the investigated samples, which presented a gel-like behavior in the linear viscoelastic region, resulting from the formation of a three-dimensional network. However, some differences could be noted, as reported in Fig. 8. The viscoelastic behavior was similar for samples A and D which presented the highest initial G' moduli, about 6 times higher than the corresponding initial G" moduli at low strain. The slight G' reduction and the high G" decrease in sample D showed how homogenization influenced collagen fiber interaction and thus the rheological properties of collagen suspensions. The effect of pepsin concentration was clearly observable and inversely proportional to samples rheological properties. In particular, G' and G" values were found to decrease with pepsin concentration increase. Indeed, sample C (pepsin concentration of 50 %) presented the lowest viscoelastic properties and G' was only three times higher than G". As regards the influence of the extraction temperature, it was clear how it significantly affected collagen suspension properties since a reduction of G' of almost three times was registered in sample E (extraction temperature of 30 ± 5 °C), compared to sample A (extraction temperature 15 ± 5 °C). All the differences in the values for the five studied samples were statistically significant ($p < 0.05$).

During the strain sweep test, G' remained constant until the oscillation stress overcame the intermolecular forces determining the linear viscoelastic region. The strain value above which G' decreased >10 % of the maximum initial value has been taken as the critical strain (γcrit), at which a polymer shows nonlinear viscoelastic behavior. This value represented the maximum shear strain that can be applied to the system keeping the condition of linear viscoelasticity. The critical strains were reported in Fig. 8 for all the analyzed samples. Once again samples A and D presented the maximum values, 8 % and 14 % respectively, while sample C was the lowest (2 %).

Statistically significant differences ($p < 0.05$) were observed also in the cohesion energy values (Fig. 8). Sample D had the highest value (28.29 kJ/m^3) indicating much stronger physical crosslinks between the polymer chains. In this case, homogenization could have shortened collagen fibers that thus interacted more and revealed a higher cohesion energy. On the contrary, sample C, which was extracted with the highest

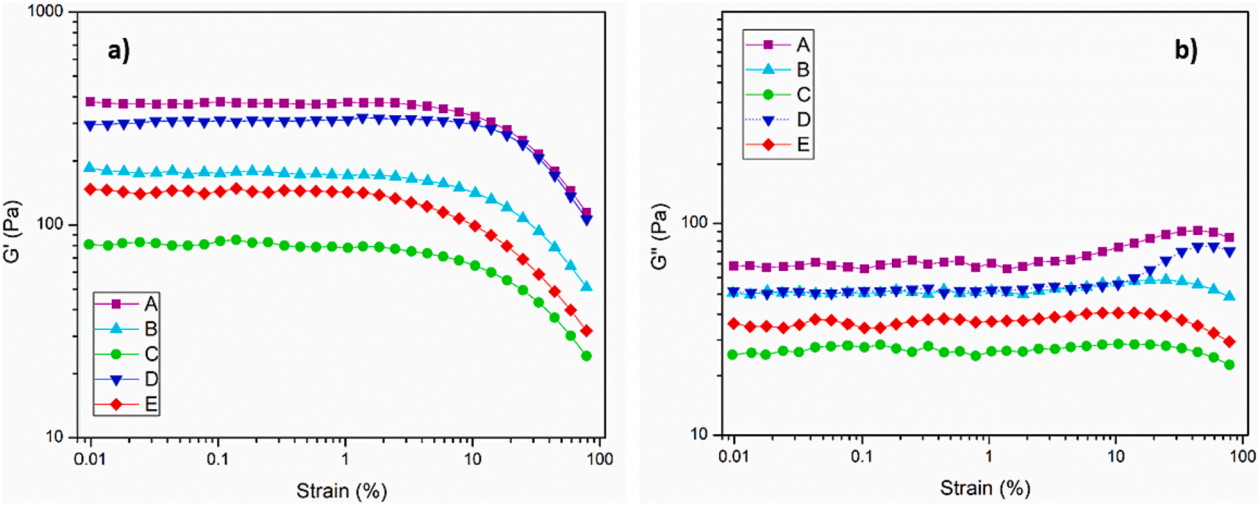

Fig. 7. Dynamic strain sweep on collagen suspensions at constant frequency (1 Hz). The evolution of the storage shear modulus (G') as a function of shear strain in a dynamic strain sweep test at 1 Hz and 20 °C revealed that G' was higher than the G" for all the investigated samples, confirming their gel-like behavior in the linear viscoelastic region.

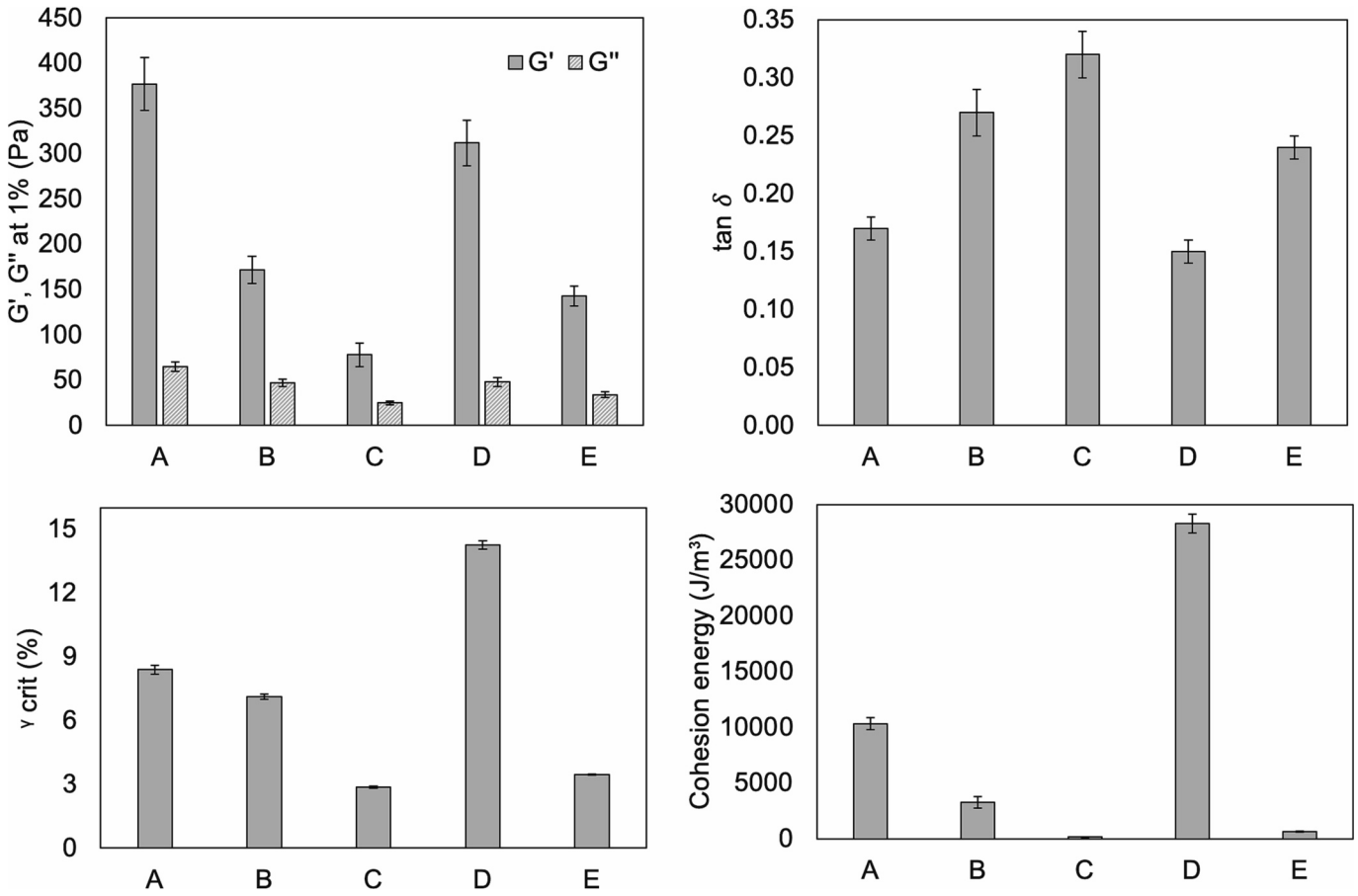

Fig. 8. Strain sweep test on collagen suspensions. Shear moduli, critical strain and cohesion energy values.

pepsin concentration, was found to be characterized by the lowest cohesion energy (0.17 kJ/m^3).

Dynamic frequency sweeps were carried out at constant shear strain within the linear viscoelastic region, where the material response is independent of the deformation magnitude. The DMA curves reported in Fig. 9 showed that G' modulus gradually increases with the frequency. Moreover, G' was higher than G" in the whole experimental frequency range with similar G' to G" ratios obtained in strain sweep tests. Therefore, all the samples behave as self-standing hydrogels, with the elastic behavior dominant compared to the viscous one. However, there are differences among sample typologies, since samples A and D were significantly ($p < 0.05$) more elastic suspensions than sample C, which present G' values 4 times higher than the corresponding G" values.

The rheological plot in Fig. 10 evidenced, for all the investigated

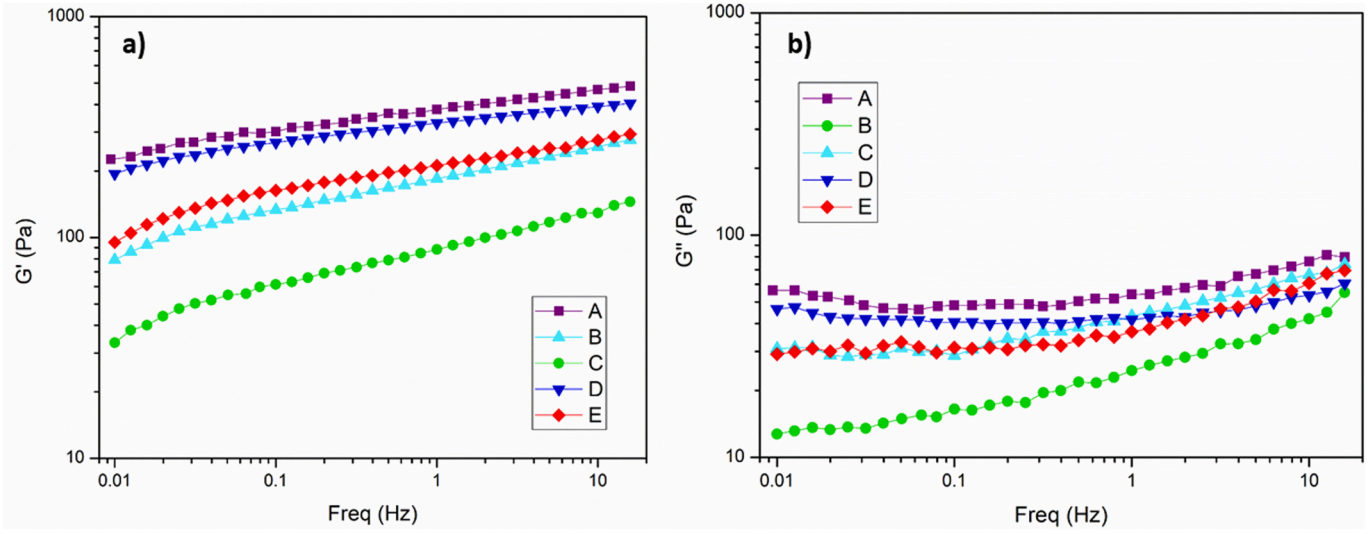

Fig. 9. Dynamic frequency sweep on collagen suspensions at constant 1 % strain. G' modulus gradually increases with the frequency. All samples behave as self-standing hydrogels, with the elastic behavior dominant on the viscous one.

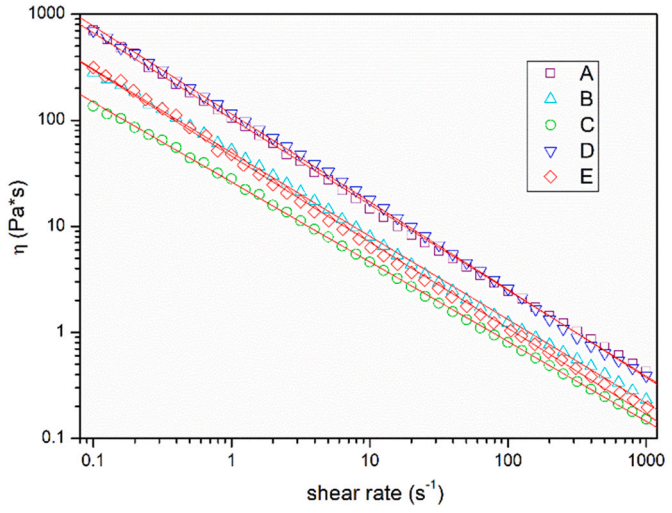

Fig. 10. Viscosity behavior of collagen suspensions as a function of shear rate. Viscosity decreases with increasing shear rate, indicating the shear thinning response typical of non-Newtonian fluids.

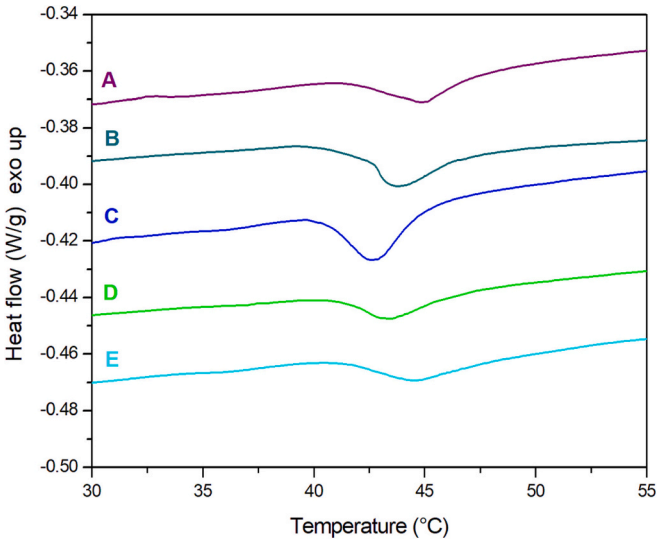

Fig. 11. DSC thermograms of collagen suspensions extracted from equine tendon. The endothermic phenomenon registered was attributed to collagen denaturation temperature, that was found to be in the range 42–45 °C.

samples, a continuous decrease in viscosity with increasing shear rate, which indicates a shear thinning response typical of non-Newtonian fluids. The viscosity values at a shear rate of 1 s^{-1} were reported in Table 3. Differences among samples were in agreement with DMA results.

The rheological curves can be fitted using the Ostwald-de Waele model, which uses a power law to describe the viscosity behavior as a function of shear rate:

$$\eta = K\dot{\gamma}^{n-1}$$

where *K* is the consistency coefficient and *n* is the flow behavior index. *K* can also be considered as the viscosity at the shear rate of 1.0 s^{-1}. The fitting parameters of rheological curves are reported in Table 3 and the fitting vurves are reported in Fig. 10. The obtained small values of the flow index (n between 0.17 and 0.25) indicated a stronger shear-thinning behavior of the suspensions. These data, together with the values of tan δ in Fig. 8 suggested a good printability and shape retention of the obtained collagen [69]. Therefore, DMA and rheological analysis reveal the potential of the obtained collagen hydrogels for 3D printing.

3.6. Thermal behavior

DSC is a powerful technique allowing to gain information about collagen thermal stability. The thermal behavior was evaluated both on collagen films and suspensions but harvested data on collagen dry films were not statistically different (Td = 46–49 °C, ΔH = 7–13 J/g). Instead, thermal transitions of collagen suspension samples were found to be significant. Thus, DSC thermograms were depicted in Fig. 11 and the relative thermal information was reported in Table 4. As expected, collagen Td was found to be about 42–44 °C, according to literature about fibrous equine tendon collagen [44]. A decrease of Td was revealed with increasing pepsin concentration, indicating collagen fiber disintegration. Indeed, the Td of sample A was significantly different from that of sample C ($p < 0.5$). Statistically significant differences were registered in the enthalpy ΔH associated with the energy required for destructing hydrogen bonds of the collagen triple helix [70].

According to other performed analyses, pepsin concentration was found to decrease collagen ΔH while temperature seemed to not affect it (compared to sample A). In particular, no statistically significant differences were registered among sample A and sample B ($p = 0.71$), while a significant reduction was observed compared to sample C. Conversely, homogenization was found to increase the ΔH value, probably because of the higher hydrogen bond interaction among fibers.

Table 3
Parameters of the power law fitting of rheological curves.

Sample	K (Pa*s^n)	n (−)	R^2
A	103.51 ± 1.76	0.19	0.999
B	49.66 ± 2.36	0.21	0.999
C	26.18 ± 1.29	0.25	0.999
D	114.82 ± 1.40	0.17	0.999
E	46.03 ± 0.84	0.19	0.999

Table 4
Denaturation temperature and enthalpy of equine collagen.

Sample	Td (°C)	ΔH (J/g)
A	44.9 ± 1.0	44.5 ± 10.1
B	43.7 ± 1.1	48.8 ± 15.9
C	42.8 ± 0.5	34.0 ± 1.0
D	43.2 ± 0.9	64.7 ± 7.6
E	44.6 ± 0.4	46.7 ± 4.0

3.7. Swelling degree

The swelling test was performed to determine the ability of materials to absorb liquids and the effects of processing on their intrinsic ability. The swelling degree allows also a qualitative measurement of the degree of hydrophilicity/hydrophobicity of the material: the higher the swelling, the more hydrophilic the material and vice versa. This test was performed on collagen films rather than on collagen suspensions because in the latter case fibers are completely swelled and their water retention ability could not be evaluated. Fig. 12 shows the degree of swelling of the investigated collagen films. In general, it can be observed that in the first 3 h all samples reached a degree of swelling of about 600–1200 % [43,71]. Sample D had the highest SD%, attributable to a higher number of hydrogen interactions with water molecules. The homogenization step could have better disassembled collagen fiber and allowed for a higher activity of pepsin, which enabled the exposure of a higher number of functional groups available for hydrogen interactions. The effect of pepsin concentration was visible in samples A-C. In particular, sample A had the lowest SD%. The low pepsin concentration and the low working temperature were probably responsible for a low activity of pepsin and thus a low exposure of functional groups. The

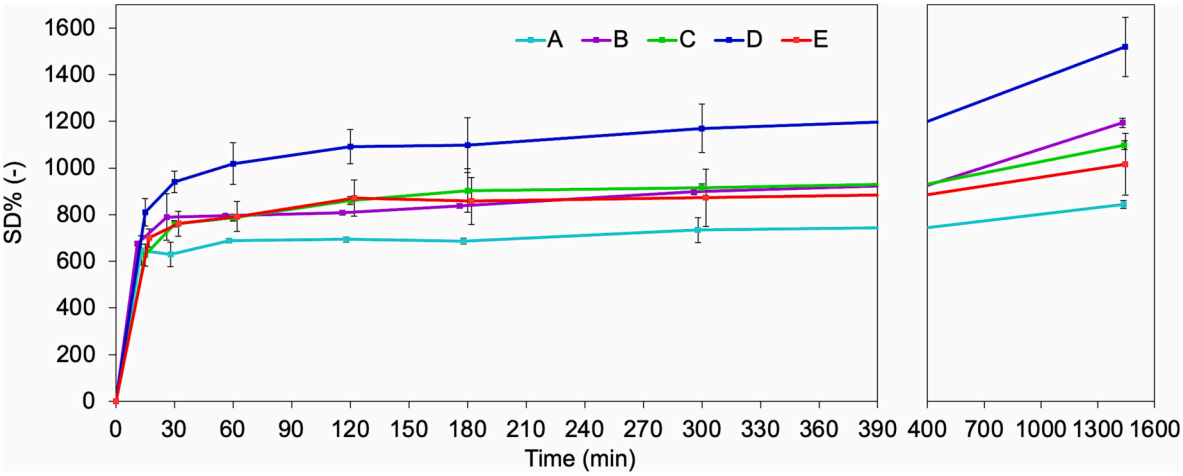

Fig. 12. Swelling degree curves of collagen films. Collagen substrates revealed to be able to uptake very fast about 600–1200 % of their weight of water in the first 3 h and then reached a plateau.

more preserved insoluble character of collagen allowed sample A to swell less than all other conditions. Accordingly, samples B and C swelled more than sample A, according to pepsin concentration, as clearly visible after 24 h of incubation. As regards the effect of the working temperature, it was found to increase sample E SD%, causing him to assume an intermediate behavior between sample A and sample D.

3.8. Mechanical properties

Tensile tests were performed to evaluate the effects of the extraction conditions on the mechanical properties of collagen films. Average stress-strain curves were reported in Fig. 13, while values of E, σ_{max} and ε_r were summarized in Table 5. As expected, all curves were characterized by three specific regions, i. e. linear elastic region, non-elastic region, and rupture region, similarly to other works reported in literature [43,71]. The effect of pepsin concentration was clearly visible in all investigated parameters. In particular, an increase in film stiffness (from 0.3 ± 0.05 MPa to 0.49 ± 0.07 MPa) was registered with pepsin concentration, accompanied by a gradual decrease of their resistance ($p < 0.05$). Indeed, while σ_{max} value almost halved (from 0.25 ± 0.05 MPa to 0.13 ± 0.01 MPa) the ε_r decreased by about one third (from 31 ± 7 % to 19 ± 3 %), compared to sample A ($p < 0.05$). Thus, the increase of pepsin concentration negatively affects collagen film properties, with a general property loss. This could be due to the fact that collagen fibers were partially gradually degraded into collagen triple-helix. The mechanical elastic contribution of fibers was reduced and prevailed the mechanical response of collagen triple-helices, detectable as matrices stiffening and reduction of maximum stress and strain at break. Similarly, homogenization was found to not affect film elastic modulus and strain at break ($p > 0.05$) but to negatively influence σ_{max}, which almost halved compared to sample A. This result could be ascribed to the fact that in sample D, fibers were almost preserved but shorter. Thus, their elastic response was not affected while the maximum stress was reduced because of their less entanglement level compared to sample A. Lastly, the temperature of the treatment significantly influenced only the elastic modulus of film E value, which reached a value of 0.55 ± 0.09 MPa.

Table 5
Shear modulus (E), stress at break (σ max) and strain at break (εr).

Sample	E (MPa)	σ_{max} (MPa)	ε_r %
A	0.30 ± 0.05	0.25 ± 0.05	31 ± 7
B	0.41 ± 0.04	0.22 ± 0.03	27 ± 4
C	0.49 ± 0.07	0.13 ± 0.01	19 ± 3
D	0.24 ± 0.09	0.12 ± 0.04	29 ± 9
E	0.55 ± 0.09	0.27 ± 0.03	24 ± 5

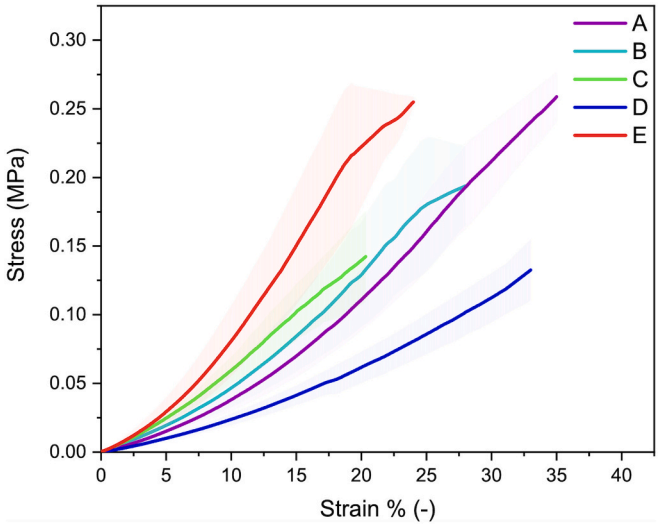

Fig. 13. Average stress-strain curves of collagen films. Beyond differences, all curves were characterized by a linear elastic region, a non-elastic region, and rupture region.

3.9. In vitro degradation resistance

The degradation resistance of collagen samples in physiological-like conditions was evaluated in order to assess the influence of extraction conditions. Their degradation rates in the presence of collagenase were almost the same and all of them were found to completely lose their structure within 4–5 h (Fig. S2). Contrarily, their degradation rates in the absence of collagenase were very different and allowed to underline structural differences among them (data from both tests were statistically significant, $p < 0.05$). As shown in Fig. 14, the degradation rates of collagen substrates were directly proportional to pepsin concentration (samples A-C). Presumably, higher concentrations of enzyme disassembled more effectively collagen fibers in collagen units (i. e., triple helices). The presence of more triple helices than fibrils could be responsible for a minor extent of intermolecular interactions and thus of less stable matrices at 37 °C. Accordingly, sample A completely degraded after 25 days, followed by sample B (that showed a behavior stackable to sample A) and sample C which degraded in 12 days.

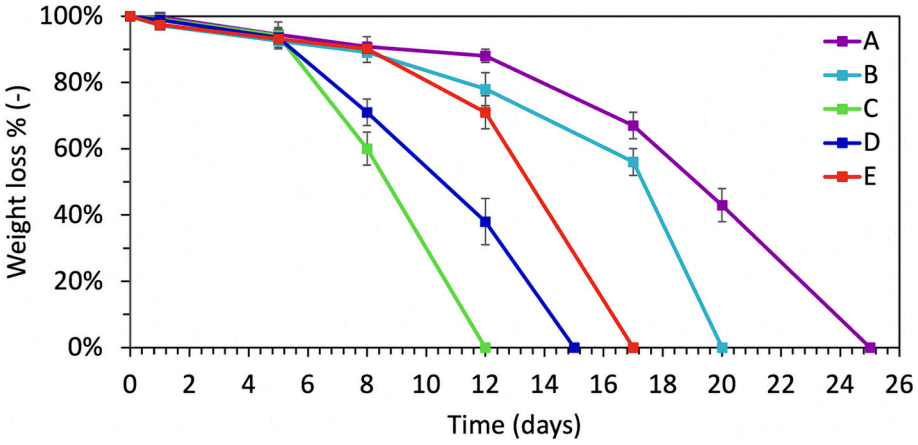

Fig. 14. Collagen film resistance in physiological-like conditions. Slight molecular/structural differences among samples allowed to tune degradation resistance in a time frame that goes from 12 days to 25 days.

Conversely, the application of a pre-homogenization before pepsin extraction (sample D) was found to reduce collagen substrate degradation resistance to 15 days, suggesting how shorter fiber reproduced a less entangled matrix that loses its 2D structure in less time compared to not homogenized samples (es. sample A). Lastly, the execution of the enzymatic treatment at 30 °C (sample E) allowed to obtain an intermediate behavior, with a complete matrix degradation after 17 days. However, our air-dried collagen film degradation resistance was found to be higher than similar horse collagen derived products, which was about 7–10 days [72].

4. Discussion and conclusion

This work focused on the effect of some parameters of the pepsin-based extraction step on the final properties of native-like fibrillar, insoluble, type I collagen in order to finely tune scaffold properties to closely mimic the tissues' hierarchical features while preserving its natural conformation. Due to this, pepsin was chosen as an enzyme for its specificity for non-helical telopeptide regions and thus for its ability to isolate collagen units (i.e., the triple helices) without disrupting their helical structure, which is fundamental for some biological processes. Moreover, pepsin specifically cleaves the peptide bonds between hydrophobic and aromatic residues [73,74], which is why it has poor collagen hydrolyzing activity.

First of all, the identity and the naiveness of the extracted protein were confirmed by SDS-PAGE, which revealed uncut type I collagen typical electrophoretic patterns thanks to the low affinity of pepsin for collagen [32,34]. The absence of low molecular weight residues confirmed the purity, the naiveness of the materials and the eligibility of the used extraction parameters for fibrous collagen isolation [44]. Then, the preservation of collagen functional groups, and thus of free -NH_2 residues, was investigated by means of the TNBS test. The almost same concentration of free amines suggested how all performed extraction processes did not alter collagen sample groups that are fundamental for the formation of intermolecular interactions. Similarly, the detection of the typical IR spectra of type I collagen, with no peak position variations, confirmed the nature of the extracted materials [21,44] and that the selected pepsin hydrolysis conditions did not affect collagen samples triple-helical structure [36]. Afterward, AFM analysis morphologically confirmed the extracted materials type since collagen fibrils with their typical D-banding (about 60–70 nm) were observed. No variations of D-banding among samples were measured, suggesting how the performed extraction processes did not affect collagen fibrillar structure but allowed to preserve it with several degrees. Indeed, selected parameters were found to influence the number of fibrils for the area unit. Collagen thermal stability was investigated by DSC analysis that revealed, for all examined conditions, the same Td at about 42–45 °C for all formulations [43,44], but different ΔH. In particular, pepsin concentration seemed to decrease collagen ΔH while temperature seemed to not affect it. Conversely, homogenization was found to increase the ΔH value, probably because of the higher hydrogen interaction among fibers.

As emerged from the aforementioned analysis, the presence of insoluble collagen fibers with their characteristic D-banding showed that not all telopeptide regions were attached by pepsin and still remained unbroken after the performed extraction protocols. Besides the low affinity of pepsin for collagen, this could be due to the inappropriate amount of enzyme or to the non-optimal enzyme working conditions. Indeed, low working temperature values revealed to be effective in isolating collagen fibers while working temperature values higher than 30 °C revealed to be suitable for the isolation of collagen triple helices, as reported by Qian et al. [34] or peptides. Moreover, it should not be neglected that pepsin's low activity could be due to the high hierarchical and strict organization of horse tendon collagen that did not make cleavage sites even accessible to the enzyme.

These results allowed thus to spot pepsin as a suitable enzyme for the extraction of native type I collagen with high conservation of its fibrillar-like structure. The modification of the pepsin-based extraction step allowed for finely tuning isolated collagen fibers properties without deeply affecting their structural conformation and thus their bioactivity. However, extraction parameters influenced the reconstituted material properties. Significant differences were observed with the rheological analysis, tensile test, and degradation resistance assay. Indeed, collagen suspensions viscoelastic properties with a shear thinning behavior were evidenced, with strong differences among samples. In particular, the effect of pepsin concentration was clearly observable and inversely proportional with samples rheological properties, while the extraction temperature reduced suspension performances by about three times. The high number of hydrogen interactions between likely shorter collagen chains, caused by the homogenization process in sample D, led to the formation of a stronger three-dimensional network compared to the other tested formulations, as revealed by the results of dynamic mechanical analysis (DMA), where the highest cohesion energy and critical strain were obtained for sample D. On the contrary, high pepsin concentrations were found to reduce collagen molecule interaction and cohesion energy. Moreover, the obtained rheological and DMA results confirmed the possibility of finely tuning the rheological and viscoelastic properties according to the desired application.

Similar results were observed with uniaxial tensile tests. Also in this case, the effect of pepsin concentration was clearly visible in all investigated parameters with an increase of film stiffness, accompanied by a gradual decrease of their resistance of two or three times. Thus, the increase of pepsin concentration negatively affected collagen film

properties, with a general properties loss. While homogenization was revealed to increase collagen suspensions properties, it negatively influenced collagen film σ_{max}, which almost halved because of the shortening of the length of the fibers.

The rheological, DMA and mechanical results suggested that an increase of pepsin concentration allowed for a higher fiber and fibril disassembly and thus higher triple helical content and exposure of functional groups. The increase of the collagen monomeric unit percentage results in higher intermolecular interactions but lower rheological/mechanical properties due to the intrinsic properties of collagen fibers partial loss. Clear was the effect of homogenization that shortened fibers length resulting in a collagenous formulation with inferior properties compared to the not-homogenized sample. However, homogenization allowed for a higher and more uniform fiber dispersion and thus more reproducible material properties. Additionally, the homogenization step could have better disassembled collagen fiber and allowed for a higher activity of pepsin, which could have enabled the exposure of a higher number of functional groups available for hydrogen interactions. Lastly, temperature was found to enhance pepsin activity, with a minor extent of fibrils and thus of native properties retain.

Results of all analyses were in accordance with samples behavior in physiological-like conditions, with a reduced resistance to degradation when higher pepsin concentrations were used, along with homogenization and a higher working temperature, according to all performed analyses. In particular, this last assay allowed to discover that extraction process parameter modulation can alter collagen substrate stability that went from 12 to 25 days, offering the possibility to choose the type of material based on the time that the final device should resist in the body before biodegrading. Additionally, our air-dried collagen film degradation resistance was found to be higher than similar horse collagen derived products [72] and other animal derived products, suggesting the particular suitability of selected extraction conditions for the manufacturing of longer lasting devices. Indeed, for example, samples C and D could be used for the development of delivery systems for the weekly controlled delivery of selected drugs, for wound dressing for non-severe wounds or for the development of sponges for guided dental bone or periodontal pocket regeneration. Sample A and B could instead be employed for the development of implantable devices for the regeneration of small part of injured tissues that require more time to regenerate (e.g., wound dressings for non-healing wounds, nerve guide for peripheral nerve regeneration, and so on). In these cases and others, it is important that the devices maintain their integrity and thus their structural functions for the time required by the regenerating tissue, and thus that they were slowly metabolized by the body's physiological enzymatic apparatus for collagen.

Apart from these applications, all sample types can be suitable for 3D printing for the development of tissues/organs 3D models with several intrinsic stiffness and half-life. Accordingly, cell behavior could be directed or customized according to the needs. Despite the reported degradation resistance may seem too low for certain applications, it should be taken into account that collagen properties could be further improved post-extraction by improving collagen concentration [80–82], by applying pre-processing modifications [21], by inducing fibrillogenesis [83–85], by crosslinking (i. e., physical, chemical, or enzymatic) [49,77–79,82,86] or by functionalizing with inhibitors of collagenase [49,75–79]. The induction of in situ silicification/mineralization [87,88] or the blending with other biomaterials [89,90] are other solutions. Nevertheless, all these modifications could be applied only post collagen extraction, allowing for a limited material properties modification. Instead, the structural changes that could be induced on collagen during the pepsin-based extraction step could allow upstream control of its properties and thus to more in depth customize its final properties in a huge variety of formulations.

Thus, acquired data allowed to correlate collagen structure at the supramolecular scale with its macro properties, confirming the possibility and the ability to tune collagen properties as needed by modifying pepsin-based extraction parameters in the collagen isolation process. In conclusion, this work evidenced how the properties of collagen-based devices could be customized by modifying processing parameters, in particular by varying their enzymatic extraction method, and to manufacture products with adjustable properties in terms of morphology, mechanics, degradation resistance without significantly affecting collagen native structure, that is of fundamental importance for cell response. The topic of modifying the properties of materials in the initial stages of the development of customized medical devices is of great interest. For this reason, future studies will be directed toward studying the impact of other process parameters on the properties of collagen and of the relative devices.

CRediT authorship contribution statement

Conceptualization, L.S., N.G., M.L.N.; methodology, N.G., M.L.N., F. L., Z.R.; software, N.G., F.R., S.B.; validation, M.L.N., Z.R.; formal analysis, N.G., F.R., Z.R.; investigation, N.G., S.B.; resources, A.S., F.L., C.M., L.S.; data curation, N.G., F.R., Z.R., S.B.; writing—original draft preparation, N.G., F.R., Z.R., S.B.; writing—review and editing, N.G., L. S., F.L., C.M.; visualization, N.G., F.L., F.R., C.M.; supervision, N.G., F.L., L.S., C.M., A.S.; project administration, L.S., A.S., F.L.; funding acquisition, A.S., F.L., C.M. All authors have read and agreed to the published version of the manuscript.

Funding

This research was funded by the projects “URORIGEN COLL – Development of an innovative collagen-based biomaterial for urethral regeneration” and “NANOCOLLAGEN - Development of nanometric collagen from waste from the fish industry” of the “Programma Regionale RIPARTI (assegni di RIcerca per riPARTire con le Imprese)” POC PUGLIA FESR-FSE 2014/2020”.

Disclaimer/publisher's note

The statements, opinions and data contained in all publications are solely those of the individual author(s) and contributor(s) and not of MDPI and/or the editor(s). MDPI and/or the editor(s) disclaim responsibility for any injury to people or property resulting from any ideas, methods, instructions or products referred to in the content

Declaration of competing interest

The authors declare no conflict of interest.

Data availability

The raw/processed data required to reproduce these findings cannot be shared at this time as the data also forms part of an ongoing study. Data will be made available on request.

Acknowledgments

None.

Appendix A. Supplementary data

Supplementary data to this article can be found online at https://doi.org/10.1016/j.ijbiomac.2023.128489.

References

[1] L. Salvatore, N. Gallo, M.L. Natali, A. Terzi, A. Sannino, M. Madaghiele, Mimicking the hierarchical organization of natural collagen: toward the development of ideal scaffolding material for tissue regeneration, Front. Bioeng. Biotechnol. 9 (2021), https://doi.org/10.3389/fbioe.2021.644595.

[2] N. Gallo, M.L. Natali, A. Sannino, L. Salvatore, An overview of the use of equine collagen as emerging material for biomedical applications, J Funct Biomater. 11 (2020) 1–27, https://doi.org/10.3390/jfb11040079.
[3] M.E. Nimni, Collagen: Biochemistry, Biomechanics, Biotechnology, CRC Press Inch, Boca Raton, FL, 1988.
[4] S. Gorgieva, V. Kokol, Collagen- vs. gelatine-based biomaterials and their biocompatibility: review and perspectives, in: Biomaterials applications for nanomedicine, InTech 2 (2011) 18–52, https://doi.org/10.5772/24118.
[5] C.H. Lee, A. Singla, Y. Lee, Biomedical applications of collagen, Int. J. Pharm. 221 (2001) 1–22, https://doi.org/10.1016/S0378-5173(01)00691-3.
[6] S. Chattopadhyay, R.T. Raines, Review collagen-based biomaterials for wound healing, Biopolymers 101 (2014) 821–833, https://doi.org/10.1002/bip.22486.
[7] E.A. Abou Neel, L. Bozec, J.C. Knowles, O. Syed, V. Mudera, R. Day, J.K. Hyun, Collagen - emerging collagen based therapies hit the patient, Adv. Drug Deliv. Rev. 65 (2013) 429–456, https://doi.org/10.1016/j.addr.2012.08.010.
[8] D.G. Wallace, J. Rosenblatt, Collagen gel systems for sustained delivery and tissue engineering, Adv. Drug Deliv. Rev. 55 (2003) 1631–1649, https://doi.org/10.1016/j.addr.2003.08.004.
[9] B. An, Y.S. Lin, B. Brodsky, Collagen interactions: drug design and delivery, Adv. Drug Deliv. Rev. 97 (2016) 69–84, https://doi.org/10.1016/j.addr.2015.11.013.
[10] C. Dong, Y. Lv, Application of collagen scaffold in tissue engineering: recent advances and new perspectives, Polymers (Basel). 8 (2016), https://doi.org/10.3390/polym8020042.
[11] I.N. Amirrah, Y. Lokanathan, I. Zulkiflee, M.F.M.R. Wee, A. Motta, M.B. Fauzi, A comprehensive review on collagen type I development of biomaterials for tissue engineering: from biosynthesis to bioscaffold, Biomedicines 10 (2022) 2307, https://doi.org/10.3390/biomedicines10092307.
[12] Z. Rajabimashhadi, N. Gallo, L. Salvatore, F. Lionetto, Collagen derived from fish industry waste: progresses and challenges, Polymers (Basel). 15 (2023) 544, https://doi.org/10.3390/polym15030544.
[13] M.D. Shoulder, R.T. Raines, Collagen structure and stability, Annu. Rev. Biochem. (2009) 929–958, https://doi.org/10.1146/annurev.biochem.77.032207.120833. COLLAGEN.
[14] H.P. Bächinger, K. Mizuno, J.A. Vranka, S.P. Boudko, Collagen formation and structure, comprehensive natural products II, Chem. Biol. 5 (2010) 469–530.
[15] A. Sorushanova, L.M. Delgado, Z. Wu, N. Shologu, A. Kshirsagar, R. Raghunath, A. M. Mullen, Y. Bayon, A. Pandit, M. Raghunath, D.I. Zeugolis, The collagen Suprafamily: from biosynthesis to advanced biomaterial development, Adv. Mater. 31 (2019) 1–39, https://doi.org/10.1002/adma.201801651.
[16] A.L. Fidler, S.P. Boudko, A. Rokas, B.G. Hudson, The triple helix of collagens – an ancient protein structure that enabled animal multicellularity and tissue evolution, J. Cell Sci. 131 (2018), https://doi.org/10.1242/jcs.203950.
[17] X. Liu, C. Zheng, X. Luo, X. Wang, H. Jiang, Recent advances of collagen-based biomaterials: multi-hierarchical structure, modification and biomedical applications, Mater. Sci. Eng. C 99 (2019) 1509–1522, https://doi.org/10.1016/j.msec.2019.02.070.
[18] K.E. Kadler, D.F. Holmes, J.A. Trotter, J.A. Chapman, Collagen fibril formation, Biochem. J. 316 (1996) 1–11, https://doi.org/10.1042/bj3160001.
[19] A. Terzi, N. Gallo, S. Bettini, T. Sibillano, D. Altamura, M. Madaghiele, L. De Caro, L. Valli, L. Salvatore, A. Sannino, C. Giannini, Sub- and supramolecular X-ray characterization of engineered tissues from equine tendon, bovine dermis and fish skin type-I collagen, Macromol Biosci. 20 (2020), https://doi.org/10.1002/mabi.202000017, 2000017.
[20] A. Terzi, E. Storelli, S. Bettini, T. Sibillano, D. Altamura, L. Salvatore, M. Madaghiele, A. Romano, D. Siliqi, M. Ladisa, L. De Caro, A. Quattrini, L. Valli, A. Sannino, C. Giannini, Effects of processing on structural, mechanical and biological properties of collagen-based substrates for regenerative medicine, Sci. Rep. 8 (2018) 1–13, https://doi.org/10.1038/s41598-018-19786-0.
[21] A. Terzi, N. Gallo, S. Bettini, T. Sibillano, D. Altamura, L. Campa, M.L. Natali, L. Salvatore, M. Madaghiele, L. De Caro, L. Valli, A. Sannino, C. Giannini, Investigations of processing–induced structural changes in horse type-i collagen at sub and supramolecular levels, Front. Bioeng. Biotechnol. 7 (2019), https://doi.org/10.3389/fbioe.2019.00203.
[22] P. Angele, J. Abke, R. Kujat, H. Faltermeier, D. Schumann, M. Nerlich, B. Kinner, C. Englert, Z. Ruszczak, R. Mehrl, R. Mueller, Influence of different collagen species on physico-chemical properties of crosslinked collagen matrices, Biomaterials 25 (2004) 2831–2841, https://doi.org/10.1016/j.biomaterials.2003.09.066.
[23] N. Davidenko, C.F. Schuster, D.V. Bax, R.W. Farndale, S. Hamaia, S.M. Best, R. E. Cameron, Evaluation of cell binding to collagen and gelatin: a study of the effect of 2D and 3D architecture and surface chemistry, J. Mater. Sci. Mater. Med. 27 (2016), https://doi.org/10.1007/s10856-016-5763-9.
[24] N. Davidenko, S. Hamaia, D.V. Bax, J.D. Malcor, C.F. Schuster, D. Gullberg, R. W. Farndale, S.M. Best, R.E. Cameron, Selecting the correct cellular model for assessing of the biological response of collagen-based biomaterials, Acta Biomater. 65 (2018) 88–101, https://doi.org/10.1016/j.actbio.2017.10.035.
[25] A.M.E. Matinong, Y. Chisti, K.L. Pickering, R.G. Haverkamp, Collagen extraction from animal skin, Biology (Basel). 11 (2022) 905, https://doi.org/10.3390/biology11060905.
[26] L. Salvatore, N. Gallo, M.L. Natali, L. Campa, P. Lunetti, M. Madaghiele, F.S. Blasi, A. Corallo, L. Capobianco, A. Sannino, Marine collagen and its derivatives: versatile and sustainable bio-resources for healthcare, Mater. Sci. Eng. C 113 (2020), 110963, https://doi.org/10.1016/j.msec.2020.110963.
[27] M.M. Schmidt, R.C.P. Dornelles, R.O. Mello, E.H. Kubota, M.A. Mazutti, A. P. Kempka, I.M. Demiate, Collagen extraction process, Int. Food Res. J. 23 (2016) 913–922.
[28] C. Ángeles-Santos, G. Aguirre-Cruz, R. Jiménez-Alvarado, A. León-López, G. Aguirre-Álvarez, Isolation and characterisation of ovine collagen hydrolysates following thermal and different enzymatic treatments, Int. Food Res. J. 27 (2020) 1038–1045.
[29] T.R. Hakim, A. Pratiwi, J. Jamhari, N.A. Fitriyanto, R. Rusman, M.Z. Abidin, D. N. Matulessy, Y. Erwanto, Extraction of collagen from the skin of Kacang goat and production of its hydrolysate as an inhibitor of angiotensin converting enzyme, tropical, Anim. Sci. J. 44 (2021) 222–228, https://doi.org/10.5398/tasj.2021.44.2.222.
[30] D.N. Matulessy, Y. Erwanto, N. Nurliyani, E. Suryanto, M.Z. Abidin, T.R. Hakim, Characterization and functional properties of gelatin from goat bone through alcalase and neutrase enzymatic extraction, Vet World. (2021) 2397–2409, doi: 10.14202/vetworld.2021.2397-2409.
[31] M. Li, L.M. Chen, B.Q. Jiang, Process optimization and characterizations of enzyme-extracted and acid-extracted collagen from scale of bighead carp, Appl. Mech. Mater. 727–728 (2015) 21–24, https://doi.org/10.4028/www.scientific.net/AMM.727-728.21.
[32] K.-H. Jung, Y.-C. Choi, J.-Y. Chun, S.-G. Min, G.-P. Hong, Effects of concentration and reaction time of trypsin, pepsin, and chymotrypsin on the hydrolysis efficiency of porcine placenta, Korean J Food Sci Anim Resour. 34 (2014) 151–157, https://doi.org/10.5851/kosfa.2014.34.2.151.
[33] A.L. Reutersward, Solubilization of pigskin and bovine tendon after pepsin and pancreatin treatment. Effect of incubation conditions and age of animal, J. Food Technol. 20 (1985) 129–143.
[34] J. Qian, Y. Okada, T. Ogura, K. Tanaka, S. Hattori, S. Ito, J. Satoh, T. Takita, K. Yasukawa, Kinetic analysis of the digestion of bovine type I collagen telopeptides with porcine pepsin, J. Food Sci. 81 (2016) C27–C34, https://doi.org/10.1111/1750-3841.13179.
[35] Y. Duan, H. Cheng, Preparation of immobilized pepsin for extraction of collagen from bovine hide, RSC Adv. 12 (2022) 34548–34556, https://doi.org/10.1039/D2RA05744A.
[36] L. Yang, X. Wu, W. Feng, T. Zhao, Y. Zhou, F. Li, Y. Zou, S. Bai, W. Wang, Optimization of enzyme-assisted extraction and characterization of collagen from Chinese sturgeon (Acipenser sturio Linnaeus) skin, Pharmacogn. Mag. 9 (2013) 32, https://doi.org/10.4103/0973-1296.117859.
[37] P. Mokrejs, D. Janacova, P. Svoboda, Three-stage extraction of gelatines from tendons of abattoir cattle: 1—reaction conditions, Appl. Biochem. Biotechnol. 168 (2012) 917–927, https://doi.org/10.1007/s12010-012-9830-5.
[38] A.R. Vidal, L.P. Duarte, M.M. Schmidt, R.L. Cansian, I.A. Fernandes, R. de Oliveira Mello, I.M. Demiate, R.C.P. Dornelles, Extraction and characterization of collagen from sheep slaughter by-products, Waste Manag. 102 (2020) 838–846, https://doi.org/10.1016/j.wasman.2019.12.004.
[39] N. Vallejos, G. González, E. Troncoso, R.N. Zúñiga, Acid and enzyme-aided collagen extraction from the byssus of Chilean mussels (Mytilus Chilensis): effect of process parameters on extraction performance, Food Biophys. 9 (2014) 322–331, https://doi.org/10.1007/s11483-014-9339-2.
[40] Y. Zhang, K. Olsen, A. Grossi, J. Otte, Effect of pretreatment on enzymatic hydrolysis of bovine collagen and formation of ACE-inhibitory peptides, Food Chem. 141 (2013) 2343–2354, https://doi.org/10.1016/j.foodchem.2013.05.058.
[41] C. Li, Z. Tian, W. Liu, G. Li, Structural properties of pepsin-solubilized collagen acylated by lauroyl chloride along with succinic anhydride, Mater. Sci. Eng. C 55 (2015) 327–334, https://doi.org/10.1016/j.msec.2015.05.055.
[42] S. Zhu, Q. Yuan, M. Yang, J. You, T. Yin, Z. Gu, Y. Hu, S. Xiong, A quantitative comparable study on multi-hierarchy conformation of acid and pepsin-solubilized collagens from the skin of grass carp (Ctenopharyngodon idella), Mater. Sci. Eng. C 96 (2019) 446–457, https://doi.org/10.1016/j.msec.2018.11.043.
[43] N. Gallo, M.L. Natali, C. Curci, A. Picerno, A. Gallone, M. Vulpi, A. Vitarelli, P. Ditonno, M. Cascione, F. Sallustio, R. Rinaldi, A. Sannino, L. Salvatore, Analysis of the physico-chemical, mechanical and biological properties of crosslinked type-I collagen from horse tendon: towards the development of ideal scaffolding material for urethral regeneration, Materials 14 (2021), https://doi.org/10.3390/ma14247648.
[44] L. Salvatore, N. Gallo, D. Aiello, P. Lunetti, A. Barca, L. Blasi, M. Madaghiele, S. Bettini, G. Giancane, M. Hasan, V. Borovkov, M.L. Natali, L. Campa, L. Valli, L. Capobianco, A. Napoli, A. Sannino, An insight on type I collagen from horse tendon for the manufacture of implantable devices, Int. J. Biol. Macromol. 154 (2020) 291–306, https://doi.org/10.1016/j.ijbiomac.2020.03.082.
[45] C.T. Prontera, N. Gallo, R. Giannuzzi, M. Pugliese, V. Primiceri, F. Mariano, A. Maggiore, G. Gigli, A. Sannino, L. Salvatore, V. Maiorano, Collagen membrane as water-based gel electrolyte for electrochromic devices, Gels 9 (2023) 310, https://doi.org/10.3390/gels9040310.
[46] O.S. Rabotyagova, P. Cebe, D.L. Kaplan, Collagen structural hierarchy and susceptibility to degradation by ultraviolet radiation, Mater. Sci. Eng. C 28 (2008) 1420–1429, https://doi.org/10.1016/j.msec.2008.03.012.
[47] H. Ju, X. Liu, G. Zhang, D. Liu, Y. Yang, Comparison of the structural characteristics of native collagen fibrils derived from bovine tendons using two different methods: modified acid-solubilized and pepsin-aided extraction, Materials 13 (2020) 358, https://doi.org/10.3390/ma13020358.
[48] N. Gallo, M.L. Natali, A. Quarta, A. Gaballo, A. Terzi, T. Sibillano, C. Giannini, G. E. De Benedetto, P. Lunetti, L. Capobianco, F.S. Blasi, A. Sicuro, A. Corallo, A. Sannino, L. Salvatore, Aquaponics-derived tilapia skin collagen for biomaterials development, Polymers (Basel). 14 (2022) 1865, https://doi.org/10.3390/polym14091865.
[49] L. Salvatore, E. Calò, V. Bonfrate, D. Pedone, N. Gallo, M.L. Natali, A. Sannino, M. Madaghiele, Exploring the effects of the crosslink density on the

physicochemical properties of collagen-based scaffolds, Polym. Test. 93 (2021), https://doi.org/10.1016/j.polymertesting.2020.106966.
[50] C.N. Grover, J.H. Gwynne, N. Pugh, S. Hamaia, R.W. Farndale, S.M. Best, R. E. Cameron, Crosslinking and composition influence the surface properties, mechanical stiffness and cell reactivity of collagen-based films, Acta Biomater. 8 (2012) 3080–3090, https://doi.org/10.1016/j.actbio.2012.05.006.
[51] P. Melo, G. Montalbano, E. Boggio, C.L. Gigliotti, C. Dianzani, U. Dianzani, C. Vitale-Brovarone, S. Fiorilli, Electrospun collagen scaffold bio-functionalized with recombinant ICOS-fc: an advanced approach to promote bone remodelling, Polymers (Basel). 14 (2022) 3780, https://doi.org/10.3390/polym14183780.
[52] D.G. Lessard, M. Ousalem, X.X. Zhu, A. Eisenberg, P.J. Carreau, Study of the phase transition of poly(N,N-diethylacrylamide) in water by rheology and dynamic light scattering, J Polym Sci B 41 (2003) 1627–1637, https://doi.org/10.1002/polb.10517.
[53] J. Cho, M.-C. Heuzey, A. Bégin, P.J. Carreau, Physical gelation of chitosan in the presence of β-glycerophosphate: the effect of temperature, Biomacromolecules 6 (2005) 3267–3275, https://doi.org/10.1021/bm050313s.
[54] N. Gallo, A. Terzi, T. Sibillano, C. Giannini, A. Masi, A. Sicuro, F.S. Blasi, A. Corallo, A. Pennetta, G.E. De Benedetto, F. Montagna, A. Maffezzoli, A. Sannino, L. Salvatore, Age-related properties of aquaponics-derived tilapia skin (Oreochromis niloticus): a structural and compositional study, Int. J. Mol. Sci. 24 (2023) 1938, https://doi.org/10.3390/ijms24031938.
[55] N.E. Ben Ammar, M. Barbouche, A.H. Hamzaoui, Historical view of hydrogel characterization, in: Hydrogels Based on Natural Polymers, Elsevier, 2020, pp. 459–479, https://doi.org/10.1016/B978-0-12-816421-1.00017-3.
[56] S. Inanc, D. Keles, G. Oktay, An improved collagen zymography approach for evaluating the collagenases MMP-1, MMP-8, and MMP-13, Biotechniques 63 (2017) 174–180, https://doi.org/10.2144/000114597.
[57] İ.E. Künili, Effects of morphometric and biochemical parameters on collagen and pepsin-solubilized collagen yields of Holothuria tubulosa (Gmelin, 1790) and Holothuria (Roweothuria) poli (Delle Chiaje, 1823), Oceanol. Hydrobiol. Stud. 51 (2022) 100–114, https://doi.org/10.26881/oahs.2022.1.09.
[58] S. Bettini, V. Bonfrate, Z. Syrgiannis, A. Sannino, L. Salvatore, M. Madaghiele, L. Valli, G. Giancane, Biocompatible collagen paramagnetic scaffold for controlled drug release, Biomacromolecules 16 (2015) 2599–2608, https://doi.org/10.1021/acs.biomac.5b00829.
[59] K.W. Sanden, A. Kohler, N.K. Afseth, U. Böcker, S.B. Rønning, K.H. Liland, M. E. Pedersen, The use of Fourier-transform infrared spectroscopy to characterize connective tissue components in skeletal muscle of Atlantic cod (Gadus morhua L.), J. Biophotonics 12 (2019), https://doi.org/10.1002/jbio.201800436.
[60] M. Carbonaro, A. Nucara, Secondary structure of food proteins by Fourier transform spectroscopy in the mid-infrared region, Amino Acids 38 (2010) 679–690, https://doi.org/10.1007/s00726-009-0274-3.
[61] R.C.G. Coelho, A.L.P. Marques, S.M. Oliveira, G.S. Diogo, R.P. Pirraco, J. Moreira-Silva, J.C. Xavier, R.L. Reis, T.H. Silva, J.F. Mano, Extraction and characterization of collagen from Antarctic and sub-Antarctic squid and its potential application in hybrid scaffolds for tissue engineering, Mater. Sci. Eng. C 78 (2017) 787–795, https://doi.org/10.1016/j.msec.2017.04.122.
[62] K.H. Sizeland, K.A. Hofman, I.C. Hallett, D.E. Martin, J. Potgieter, N.M. Kirby, A. Hawley, S.T. Mudie, T.M. Ryan, R.G. Haverkamp, M.H. Cumming, Nanostructure of electrospun collagen: do electrospun collagen fibers form native structures? Materialia (Oxf). 3 (2018) 90–96, https://doi.org/10.1016/j.mtla.2018.10.001.
[63] G. Tronci, A. Doyle, S.J. Russel, D.J. Wood, Triple-helical collagen hydrogels via covalent aromatic functionalization with 1,3-Phenylenediacetic acid, J. Mater. Chem. B Mater. Biol. Med. 1 (2013) 5478–5488.
[64] M.B. Fauzi, Y. Lokanathan, B.S. Aminuddin, B.H.I. Ruszymah, S.R. Chowdhury, Ovine tendon collagen: extraction, characterisation and fabrication of thin films for tissue engineering applications, Mater. Sci. Eng. C 68 (2016) 163–171, https://doi.org/10.1016/j.msec.2016.05.109.
[65] L.C. Gallo, M. Madaghiele, L. Salvatore, A. Barca, S. Scialla, S. Bettini, L. Valli, T. Verri, V. Bucalá, A. Sannino, Integration of PLGA microparticles in collagen-based matrices: tunable scaffold properties and interaction between microparticles and human epithelial-like cells, international journal of polymeric materials and polymeric, Biomaterials 69 (2020) 137–147, https://doi.org/10.1080/00914037.2018.1552857.
[66] L.C. Sow, Y.R. Peh, B.N. Pekerti, C. Fu, N. Bansal, H. Yang, Nanostructural analysis and textural modification of tilapia fish gelatin affected by gellan and calcium chloride addition, LWT Food Sci. Technol. 85 (2017) 137–145, https://doi.org/10.1016/j.lwt.2017.07.014.
[67] A. Stylianou, Assessing collagen D-band periodicity with atomic force microscopy, Materials 15 (2022) 1608, https://doi.org/10.3390/ma15041608.
[68] A. Stylianou, D. Yova, Atomic force microscopy investigation of the interaction of low-level laser irradiation of collagen thin films in correlation with fibroblast response, Lasers Med. Sci. 30 (2015) 2369–2379, https://doi.org/10.1007/s10103-015-1823-5.
[69] F. Garcia-Villen, A. Guembe, J.M. Rey, T. Zúñiga, S. Ruiz-Alonso, L. Saenz-del-Burgo, J.M. Izco, J.I. Recalde, J. Luis Pedraz, Characterization and assessment of new fibrillar collagen inks and bioinks for 3D printing and bioprinting, Int J Bioprint. (2023), https://doi.org/10.18063/ijb.712.
[70] C. Ding, M. Zhang, K. Wu, G. Li, The response of collagen molecules in acid solution to temperature, Polymer (Guildf). 55 (2014) 5751–5759, https://doi.org/10.1016/j.polymer.2014.09.011.
[71] S. Bose, S. Li, E. Mele, C.J. Williams, V.V. Silberschmidt, Stability and mechanical performance of collagen films under different environmental conditions, Polym. Degrad. Stab. 197 (2022), 109853, https://doi.org/10.1016/j.polymdegradstab.2022.109853.
[72] M. Vallecillo-Rivas, M. Toledano-Osorio, C. Vallecillo, M. Toledano, R. Osorio, The collagen origin influences the degradation kinetics of guided bone regeneration membranes, Polymers (Basel). 13 (2021) 3007, https://doi.org/10.3390/polym13173007.
[73] T. Kageyama, Role of S'1 loop residues in the substrate specificities of pepsin a and Chymosin, Biochemistry 43 (2004) 15122–15130, https://doi.org/10.1021/bi048440g.
[74] J.S. Fruton, The Specificity and Mechanism of Pepsin Action, 1970, pp. 401–443, https://doi.org/10.1002/9780470122785.ch9.
[75] T.S. Thring, P. Hili, D.P. Naughton, Anti-collagenase, anti-elastase and anti-oxidant activities of extracts from 21 plants, BMC Complement. Altern. Med. 9 (2009) 27, https://doi.org/10.1186/1472-6882-9-27.
[76] F. Yu, M.L. Luo, R.C. Xu, L. Huang, W. Zhou, J. Li, F.R. Tay, L.N. Niu, J.H. Chen, Evaluation of a collagen-reactive monomer with advanced bonding durability, J. Dent. Res. 99 (2020) 813–819, https://doi.org/10.1177/0022034520913540.
[77] M. Madaghiele, E. Calò, L. Salvatore, V. Bonfrate, D. Pedone, M. Frigione, A. Sannino, Assessment of collagen crosslinking and denaturation for the design of regenerative scaffolds, J. Biomed. Mater. Res. A 104 (2016) 186–194, https://doi.org/10.1002/jbm.a.35554.
[78] S.D. Gorham, N.D. Light, A.M. Diamond, M.J. Willins, A.J. Bailey, T.J. Wess, N. J. Leslie, Effect of chemical modifications on the susceptibility of collagen to proteolysis. II. Dehydrothermal crosslinking, Int. J. Biol. Macromol. 14 (1992) 129–138, https://doi.org/10.1016/S0141-8130(05)80002-9.
[79] I. Rault, V. Frei, D. Herbage, Evaluation of Different Chemical Methods for Cross-Linking Collagen Gel, Films and Sponges, 1996.
[80] C.M. Tierney, M.G. Haugh, J. Liedl, F. Mulcahy, B. Hayes, F.J. O'Brien, The effects of collagen concentration and crosslink density on the biological, structural and mechanical properties of collagen-GAG scaffolds for bone tissue engineering, J. Mech. Behav. Biomed. Mater. 2 (2009) 202–209, https://doi.org/10.1016/j.jmbbm.2008.08.007.
[81] E. Suesca, A.M.A. Dias, M.E.M. Braga, H.C. de Sousa, M.R. Fontanilla, Multifactor analysis on the effect of collagen concentration, cross-linking and fiber/pore orientation on chemical, microstructural, mechanical and biological properties of collagen type I scaffolds, Mater. Sci. Eng. C 77 (2017) 333–341, https://doi.org/10.1016/j.msec.2017.03.243.
[82] V. Perez-Puyana, A. Romero, A. Guerrero, Influence of collagen concentration and glutaraldehyde on collagen-based scaffold properties, J. Biomed. Mater. Res. A 104 (2016) 1462–1468, https://doi.org/10.1002/jbm.a.35671.
[83] G.D. Pins, F.H. Silver, A self-assembled collagen scaffold suitable for use in soft and hard tissue replacement, Mater. Sci. Eng. C 3 (1995) 101–107, https://doi.org/10.1016/0928-4931(95)00109-3.
[84] A. Jean, G.C. Engelmayr, Anisotropic collagen Fibrillogenesis within microfabricated scaffolds: implications for biomimetic tissue engineering, Adv. Healthc. Mater. 1 (2012) 112–116, https://doi.org/10.1002/adhm.201100017.
[85] M. Achilli, D. Mantovani, Tailoring mechanical properties of collagen-based scaffolds for vascular tissue engineering: the effects of pH, temperature and ionic strength on gelation, Polymers (Basel). 2 (2010) 664–680, https://doi.org/10.3390/polym2040664.
[86] L. Gu, T. Shan, Y. Ma, F.R. Tay, L. Niu, Novel biomedical applications of crosslinked collagen, Trends Biotechnol. 37 (2019) 464–491, https://doi.org/10.1016/j.tibtech.2018.10.007.
[87] J. Sun, K. Jiao, Q. Song, C. Ma, C. Ma, F.R. Tay, L. Niu, J. Chen, Intrafibrillar silicified collagen scaffold promotes in-situ bone regeneration by activating the monocyte p38 signaling pathway, Acta Biomater. 67 (2018) 354–365, https://doi.org/10.1016/j.actbio.2017.12.022.
[88] K. Jiao, L. Niu, C. Ma, X. Huang, D. Pei, T. Luo, Q. Huang, J. Chen, F.R. Tay, Complementarity and uncertainty in intrafibrillar mineralization of collagen, Adv. Funct. Mater. 26 (2016) 6858–6875, https://doi.org/10.1002/adfm.201602207.
[89] J. Zhu, Z. Li, Y. Zou, G. Lu, A. Ronca, U. D'Amora, J. Liang, Y. Fan, X. Zhang, Y. Sun, Advanced application of collagen-based biomaterials in tissue repair and restoration, Journal of Leather Science and Engineering. 4 (2022) 30, https://doi.org/10.1186/s42825-022-00102-6.
[90] A. Sionkowska, Collagen blended with natural polymers: recent advances and trends, Prog. Polym. Sci. 122 (2021), 101452, https://doi.org/10.1016/j.progpolymsci.2021.101452.